Quantum mechanics–molecular dynamics approach to the interpretation of x-ray absorption spectra

A Kuzmin[1] and R A Evarestov[2]

[1] Institute of Solid State Physics, University of Latvia, Kengaraga Street 8,
LV-1063 Riga, Latvia
[2] Department of Quantum Chemistry, St Petersburg State University,
26 Universitetskiy Prospekt, Stary Peterhof 198504, Russia

E-mail: a.kuzmin@cfi.lu.lv

Abstract
The quantum mechanics–molecular dynamics approach to the simulation of configuration-averaged EXAFS spectra is proposed, and its application is discussed for the example of the Ti K-edge EXAFS spectrum in cubic perovskite $SrTiO_3$. Proper use of *ab initio* quantum mechanics allows a number of empirical parameters, used in the molecular dynamics simulation, to be reduced, whereas the molecular dynamics allows us to account for temperature effects. All together, the approach provides a way of accounting for static and dynamic disorder in EXAFS signals from the coordination shells above the first one, where many-atom (multiple-scattering) effects are often important.

(Some figures in this article are in colour only in the electronic version)

1. Introduction

X-ray absorption spectroscopy (XAS) at synchrotron radiation sources is a modern structural tool providing information on the local atomic and electronic structure around an atom of a particular type. The size of the region, probed by XAS, depends on the degree of thermal and static disorder present in a compound and is typically about 3–10 Å around the absorbing atom. While a reliable theory of x-ray absorption spectra (EXAFS/XANES) has been developed in the past [1], there is still a lack of accurate accounting for disorder effects, in particular, beyond the first coordination shell—in the region, where the so-called multiple-scattering (MS) effects [1, 2], depending on many-atom distributions, contribute. This problem strongly limits the conventional routine analysis and interpretation of the EXAFS signals to the first coordination shell.

Currently, the problem of disorder in EXAFS is theoretically considered within two approaches: one relies on a distribution of instantaneous interatomic distances contributing to the multiple-scattering paths [1], whereas another one uses a configurational average of the EXAFS signals over n-atom distributions [3, 4].

In the first case, realized within the FEFF code [5], the treatment of thermal and structural disorder is based on phenomenological models, such as the correlated Einstein and Debye models, Gaussian or cumulant approximations [1]. However, a few attempts to use more rigorous approaches, based on semiempirical Hamiltonians and the *ab initio* density functional method [6] or the equation-of-motion method [7], have also been performed.

In the second approach, implemented in the GNXAS code [4, 8], the configurational averages of the EXAFS signals are calculated using the low-order Taylor expansion for amplitude and phase of the EXAFS signal, assuming small disorder.

In practice, an even better approach can be implemented using the FEFF or GNXAS code to generate a configuration-averaged EXAFS signal from a set of atomic configurations, which can be obtained from molecular dynamics (MD), Monte Carlo (MC) or reverse Monte Carlo (RMC) simulations [9–16]. Note that, in the first two methods, MD and MC, the interaction between atoms is taken into account through the use of interatomic potentials, while in the RMC technique no interatomic interactions are assumed.
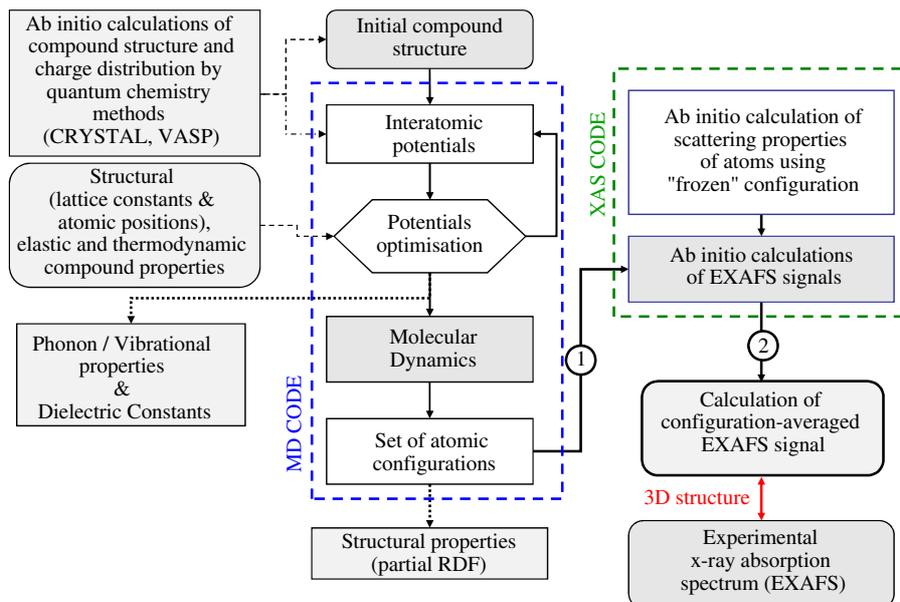
Figure 1. Scheme of combined quantum mechanics and molecular dynamics (QCMD) approach to the x-ray absorption spectra simulation. See the text for details.

In this work, we present a recently developed approach, used to simulate configuration-averaged x-ray absorption spectra, based on a combination of quantum mechanics and molecular dynamics (QM–MD) methods. The approach allows straightforward accounting for both thermal and structural disorder within the MS contributions. The present state-of-the-art of the method is illustrated for the example of the Ti K-edge EXAFS signal in the perovskite-type $SrTiO_3$ compound, taken from [17].

2. Simulation method

The scheme of a combined quantum mechanics–molecular dynamics (QCMD) approach to the x-ray absorption spectra simulation is shown in figure 1. It can be separated into several steps, which technically can be implemented in different ways.

One starts from the atomic structure of a compound, which should be obtained from a diffraction experiment or calculated by one of the *ab initio* quantum-chemistry codes, such as, for example, the LCAO (linear combination of atomic orbitals) code CRYSTAL [18] or PW (plane wave) code VASP [19]. In the latter case, one also obtains information on the atomic charges. In LCAO calculations atomic charges are found by Mulliken population analysis, whereas in PW calculations Bader atomic charges are used. The calculated atomic charges can be used further for fitting the empirical interatomic potentials, thus reducing the number of free unknown parameters.

When the atomic structure of the compound is defined, one needs to choose a set of interatomic potentials and perform their optimization by refining the potential parameters to some physical properties of the compound. These can be structural parameters (such as lattice constants and atomic fractional coordinates within the unit cell), elastic constants and thermodynamic properties. To solve this task, we use the GULP code [20, 21], which incorporates the interatomic potentials optimization procedure. Note that the thus obtained interatomic potentials should allow accurate reproduction of the structural parameters (normally to better than ±0.01–0.02 Å) to make further comparison of calculated and experimental EXAFS signals meaningful. After refinement of interatomic potentials, the vibrational frequencies, phonon dispersions and density of vibrational states can be calculated and compared with the results of Raman scattering, infrared spectroscopy or inelastic neutron scattering, when available.

In the next step, the molecular dynamics simulation should be performed for the temperature of the EXAFS experiment. Note that, when classical MD simulations are made, as in the case of the GULP code [20, 21], one should take care that the simulation temperature is high enough for classical dynamics to be valid. As a result of the MD simulation, one obtains a set of instantaneous atomic configurations (compound structure 'snapshots'). These can be immediately used to calculate the partial radial distribution functions (RDFs), which can be compared with those calculated from the diffraction data to exclude the unreliable evolution of the compound structure during the MD run.

To realize the next step, two computer codes, EDAGULP and EDACA, were developed within the EDA project [22]. These are used to perform the configuration-averaged EXAFS calculation using the *ab initio* multiple-scattering (MS) code FEFF8 [5] and the results of the MD simulations by GULP [20, 21]. The first code EDAGULP converts the output of the MD GULP run into that required by the EDACA code and also calculates partial RDFs for further analysis. The EDACA code is used to perform a repeated automatic run of the FEFF8 code for each of the atomic configurations, extracted from the MD simulation, and to calculate the configuration-averaged EXAFS signal. Note that the input file required by the FEFF code is automatically generated on the fly by the EDACA code.

Table 1. Parameters of the Born–Mayer (from [24]) and Coulomb potentials, used in the MD calculations of cubic $SrTiO_3$ ($a = 3.905$ Å [25, 26]).

Pairs of atoms	A (eV)	ρ (Å)	
Sr–O	1 769.51	0.319 894	
Ti–O	14 567.4	0.197 584	
O–O	6 249.17	0.231 472	

Atoms	Z (e)	Z_{LCAO} (e)	Z (e)
Sr	1.84	1.84	1.84
Ti	1.85	2.36	3.02
O	−1.23	−1.40	−1.62

Such an approach is rather time-consuming computationally, since the number of atomic configurations, required to get a good average, is normally about a few thousand. However, it allows the final result to be obtained in a reasonable time, ranging from a few hours up to one day on a modern PC compatible computer. Since EXAFS calculations for each of the atomic configurations can be performed independently, this step is easily parallelizable and thus can benefit from modern multi-core cluster computers. The full simulation scheme (figure 1) is currently implemented at the 'LASC' cluster-type computer at ISSP (Riga) [31].

The simulated configuration-averaged EXAFS signal accounts for thermal disorder and can be directly compared with the experimental one, taking into account the size of the MD box, which determines the most distant coordination shell contributing to the EXAFS signal. Further we provide an example of the application of the above-discussed scheme to the Ti K-edge EXAFS in perovskite $SrTiO_3$. Let us also note that, while here we discuss only the EXAFS simulation, the same scheme can be applied to the calculation of the x-ray absorption near-edge structure (XANES): however, this task is much more heavy computationally due to the time required to calculate the XANES signal for a single atomic configuration.

3. Computational details

The quantum mechanics calculation of cubic $SrTiO_3$ was performed by *ab initio* CRYSTAL06 code [18] within the linear combination of atomic orbitals (LCAO) approximation and the hybrid Hartree–Fock (HF) density functional theory (DFT) approach with a B3PW exchange–correlation functional [23]. The calculated Mulliken effective atomic charges $Z_{Sr} = 1.84$, $Z_{Ti} = 2.36$ and $Z_O = -1.40$ were used further in the MD simulations.

The MD simulations of $SrTiO_3$ were performed in the *NVT* ensemble using the rigid-ion vibrational model within the quasiharmonic approximation, as implemented in the GULP code [20, 21]. The short-range pairwise repulsive interactions Sr–O, Ti–O and O–O (table 1) were described by the Born-Mayer potential $U(r) = A \exp(-r/\rho)$ acting over the range of 0–15 Å. The long-range Coulomb interactions were evaluated using the Ewald summation method [27] with three effective charges of strontium (Z_{Sr}), titanium (Z_{Ti}) and oxygen (Z_O) ions. The requirement of charge neutrality imposes that $Z_{Sr} + Z_{Ti} + 3Z_O = 0$. The values of the charges were first taken from
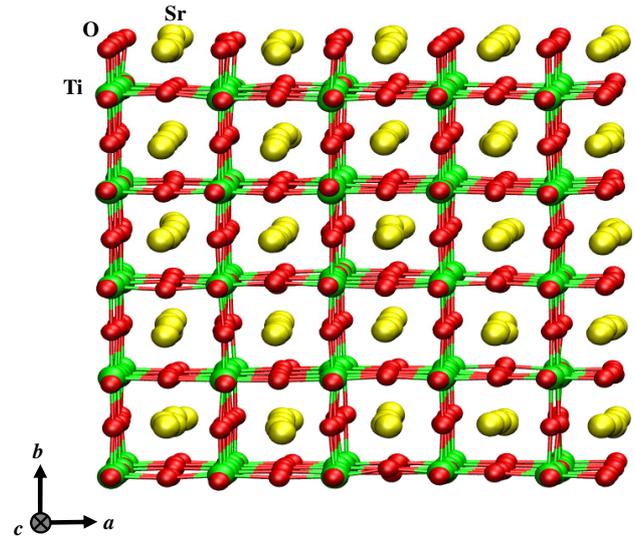

Figure 2. Snapshot of the $5 \times 5 \times 5$ supercell of $SrTiO_3$ used in the MD simulation.

the LCAO calculations, but the influence of Ti and O charge variation was also studied.

The simulations were performed for three different MD boxes (figure 2) with periodic boundary conditions. They were constructed based on the supercells composed of 9 ($3 \times 3 \times 3$), 125 ($5 \times 5 \times 5$) or 343 ($7 \times 7 \times 7$) unit cells, which contain 135, 625 and 1715 atoms, respectively. The integration of Newton's equations was done by the leapfrog Verlet method. In each simulation, the structure was equilibrated at 300 K, corresponding to the temperature of the EXAFS experiment [17], and a set of instantaneous atomic configurations was accumulated during the production run of time length 20–80 ps with a time step of 1 fs. The number of recorded configurations, used further in the EXAFS calculations, were between 1000 and 4000.

The total EXAFS signals were generated for each configuration by the FEFF8 code [5] taking into account all multiple-scattering (MS) contributions with the half-path length below 5 Å, which covers the range up to the fourth titanium coordination shell, composed of 24 oxygen atoms. At the first step of the MS calculations, the scattering potentials and phase shifts should be evaluated for all significantly different atoms in the structure [5]. In our case, since one has a large number of slightly different atomic configurations, two approaches to this problem are possible: (i) one can perform the calculations for the average configuration and neglect a variation of the scattering potentials due to thermal vibrations or (ii) one can recalculate the scattering potentials at each MD time step. Here we used the first approach to reduce significantly the computation time, and we also believe that this approximation is generally good enough in the EXAFS region for $k \geqslant 2$ Å^{-1}. Thus, the scattering potentials and phase shifts were calculated only once for a cluster with the radius of 8 Å, having the structure of cubic $SrTiO_3$ and centered at the Ti atom. The complex exchange–correlation Hedin–Lundqvist potential and default values of muffin-tin radii, as provided within the FEFF8 code [5], were used. The value of the
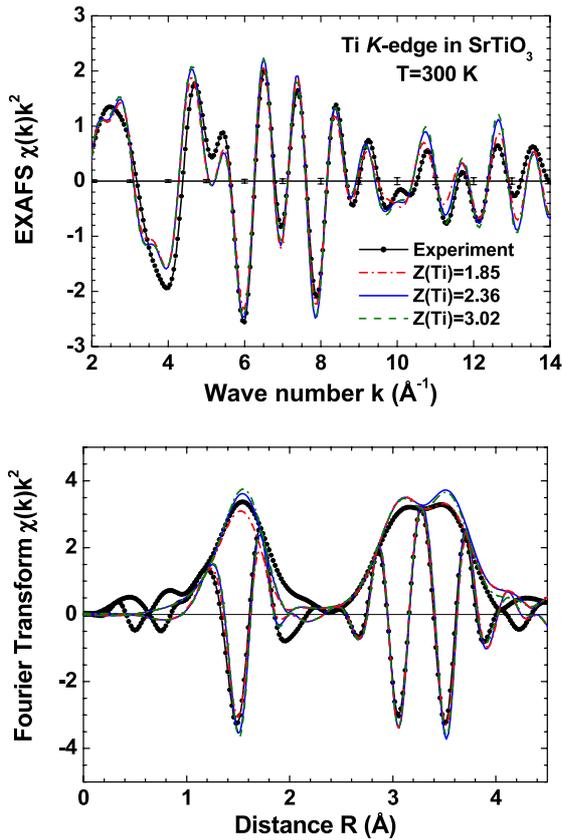
Figure 3. Effect of titanium ion charges on calculated EXAFS $\chi(k)k^2$ signals (upper panel) and their Fourier transforms (lower panel) for SrTiO$_3$ in the range up to the fourth coordination shell. Dashed–dotted curve corresponds to $Z_{\mathrm{Ti}} = 1.85$, solid—$Z_{\mathrm{Ti}} = 2.36$ and dashed—$Z_{\mathrm{Ti}} = 3.02$ (see also section 3). The experimental signals (from [17]) are shown by solid circles. Note that the Fourier transforms are not corrected by the phase shift, therefore the peak positions differ from crystallographic values. The error bars for experimental EXAFS signal are also shown. See the text for calculation details.
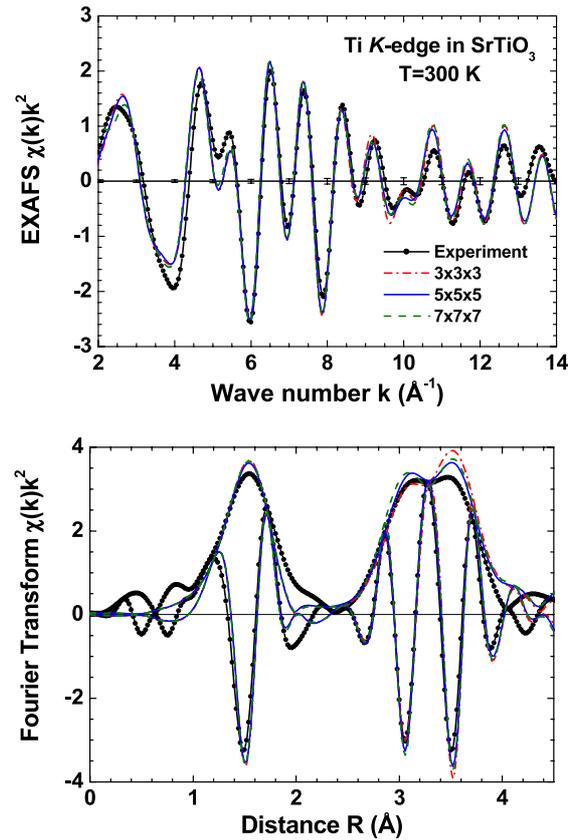
Figure 4. Effect of supercell size on calculated EXAFS $\chi(k)k^2$ signals (upper panel) and their Fourier transforms (lower panel) for SrTiO$_3$ in the range up to the fourth coordination shell. Dashed–dotted curve corresponds to supercell size $3 \times 3 \times 3$, solid—$5 \times 5 \times 5$ and dashed—$7 \times 7 \times 7$. The experimental signals (from [17]) are shown by solid circles. Note that the Fourier transforms are not corrected by the phase shift, therefore the peak positions differ from crystallographic values. The error bars for experimental EXAFS signal are also shown. See the text for calculation details.

amplitude reduction factor S_0^2 due to many-body effects was set to 0.67, as was found in [17].

4. Results

The Ti K-edge EXAFS spectra in SrTiO$_3$ and their Fourier transforms (FT), calculated using the approach described in the previous sections, are shown in figures 3 and 4, respectively. Note that no fitting parameters have been used in the calculations. In general, the agreement between the experimental and theoretical configuration-averaged EXAFS signals is good. However, the difference between the two EXAFS signals is larger than the experimental error bars. Further improvements are possible by optimizing the parameters of interatomic potentials to fit the EXAFS signal— this procedure is under development.

We are able to reproduce rather well both the amplitude and phase of the EXAFS and FT signals in the range up to 4 Å around the central Ti atom. This region corresponds to the first four coordination shells and includes also the contributions from the multiple-scattering (MS) effects within the first

(six oxygen) and third (six titanium) coordination shells [28]. Note that the MS signals, generated within the linear O–Ti$_0$– O and Ti$_0$–O–Ti (Ti$_0$ is the absorbing atom) atomic chains, are known [29, 30] to produce the largest contributions to the EXAFS signal and are also sensitive to the respective bonding angles. Thus, the first peak in FT at about 1.5 Å corresponds to six oxygen atoms in the first shell. The second peak at about 3.1 Å is due to eight strontium atoms in the second shell plus the MS contribution from the first shell. The third peak at about 3.5 Å originates from six titanium atoms in the third shell, including respective MS contributions, and 24 oxygen atoms in the fourth shell.

In figure 3 we show the influence of the Ti atomic charge on the configuration-averaged EXAFS signal. One can see that small but significant variations of the Ti charge from the value $Z_{\mathrm{Ti}} = 2.36$, obtained in the LCAO calculation, down to 1.85 and up to 3.02 does not crucially influence the result. The weak sensitivity of the EXAFS signal to the atom's charge means that the atomic charge should not be used in the potential optimization procedure, but can be determined from *ab initio* calculations, as suggested in our scheme in figure 1. More,

it means that the relatively small differences in Mulliken and Bader atomic charges can be ignored in the Coulomb part of the interatomic potentials.

The influence of the supercell size on the configuration-averaged EXAFS signal is shown in figure 4. Note that for the smallest supercell, having a size of $3 \times 3 \times 3$ unit cells, half of its linear dimension $3a/2 = 5.86$ Å ($a = 3.905$ Å is the lattice parameter of $SrTiO_3$ [25, 26]) is larger than the size (up to 4 Å) of the region compared in FT. Therefore, a small difference in the total EXAFS signal, observed mainly in the amplitude of the peaks at 3.1 and 3.5 Å, can be explained by the interaction between the atoms of the central supercell and their periodic images in the neighboring cells. Comparing the results for three supercells, one can see that, when the supercell size increases, this effect decreases. In fact, the EXAFS signals for the supercells, having sizes $5 \times 5 \times 5$ and $7 \times 7 \times 7$ unit cells, are close. This means that the $5 \times 5 \times 5$ supercell size is already sufficient in our case to obtain reliable results up to the fourth coordination shell.

5. Conclusions

In this work we have demonstrated the application of the QMMD approach to the simulation of configuration-averaged EXAFS spectra for the example of cubic perovskite $SrTiO_3$.

The use of *ab initio* calculations allows the number of empirical parameters to be reduced in the molecular dynamics simulation, whereas the molecular dynamics allows the temperature effects to be taken into account. All together this approach provides a solution to the currently open problem of static and dynamic disorder in EXAFS signals from the coordination shells beyond the first one, where many-atom (multiple-scattering) effects are important.

We also believe that our approach opens the direct way for interpretation of EXAFS spectra in nanocrystalline materials, taking into account their 'true' structure and dynamics, without any need for the oversimplified models currently being used. Finally, a refinement of the interatomic potentials based on the EXAFS spectra, i.e. the solution of the inverse problem, can be also performed: however, this task is very heavy computationally. This work is in progress.

Acknowledgment

References

[1] Rehr J J and Albers R C 2000 *Rev. Mod. Phys.* **72** 621
[2] Ravel B 2005 *J. Alloys Compounds* **401** 118
[3] Benfatto M, Natoli C R and Filipponi A 1989 *Phys. Rev.* B **40** 9626
[4] Filipponi A, Di Cicco A and Natoli C R 1995 *Phys. Rev.* B **52** 15122
[5] Ankudinov A L, Ravel B, Rehr J J and Conradson S D 1998 *Phys. Rev.* B **58** 7565
[6] Dimakis N and Bunker G 1998 *Phys. Rev.* B **58** 2467
[7] Poiarkova A V and Rehr J J 1999 *Phys. Rev.* B **59** 948
[8] Filipponi A and Di Cicco A 1995 *Phys. Rev.* B **52** 15135
[9] Winterer M 2000 *J. Appl. Phys.* **88** 5635
[10] McGreevy R L 2001 *J. Phys.: Condens. Matter* **13** R877
[11] Merkling P J, Muñoz-Páez A, Pappalardo R R and Sánchez M E 2001 *Phys. Rev.* B **64** 092201
[12] Cabaret D, Le Grand M, Ramos A, Flank A M, Rossano S, Galoisy L, Calas G and Ghaleb D 2001 *J. Non-Cryst. Solids* **289** 1
[13] Okamoto Y 2004 *Nucl. Instrum. Methods Phys. Res.* A **526** 572
[14] Farges F, Lefrère Y, Rossano S, Berthereau A, Calas G and Brown G E Jr 2004 *J. Non-Cryst. Solids* **344** 176
[15] Di Cicco A and Trapananti A 2005 *J. Phys.: Condens. Matter* **17** S135
[16] Ferlat G, Soetens J C, SanMiguel A and Bopp P A 2005 *J. Phys.: Condens. Matter* **17** S145
[17] Vračar M, Kuzmin A, Merkle R, Purans J, Kotomin E A, Maier J and Mathon O 2007 *Phys. Rev.* B **76** 174107
[18] Dovesi R *et al* 2006 *Crystal06. User's Manual* University of Turin
[19] Kresse G and Furthmuller J 2007 *VASP the Guide* Universität Wien
[20] Gale J D 1996 *Phil. Mag.* B **73** 3
[21] Gale J D and Rohl A L 2003 *Mol. Simul.* **9** 291
[22] Kuzmin A 1995 *Physica* B **208/209** 175
[23] Alexandrov V E, Maier J and Evarestov R A 2008 *Phys. Rev.* B **77** 075111
[24] Thomas B S, Marks N A and Begg B D 2005 *Nucl. Instrum. Methods Phys. Res.* B **228** 288
[25] Meyer G M, Nelmes R J and Hutton J 1978 *Ferroelectrics* **21** 461
[26] Howard S A, Yau J K and Anderson H U 1989 *J. Appl. Phys.* **65** 1492
[27] Ewald P P 1921 *Ann. Phys.* **64** 253
[28] Fischer M, Lahmar A, Maglione M, Sanmiguel A, Itié J P, Polian A and Baudelet F 1994 *Phys. Rev.* B **49** 12451
[29] Kuzmin A, Purans J, Benfatto M and Natoli C R 1993 *Phys. Rev.* B **47** 2480
[30] Kuzmin A and Purans J 1993 *J. Phys.: Condens. Matter* **5** 9423
[31] Kuzmin A 2006 *Latv. J. Phys. Tech. Sci.* **2** 7